Search for the $X(4140)$ state in $B^+ \to J/\psi\phi K^+$ decays

R. Aaij,[38] C. Abellan Beteta,[33,n] B. Adeva,[34] M. Adinolfi,[43] C. Adrover,[6] A. Affolder,[49] Z. Ajaltouni,[5] J. Albrecht,[35] F. Alessio,[35] M. Alexander,[48] G. Alkhazov,[27] P. Alvarez Cartelle,[34] A. A. Alves, Jr.,[22] S. Amato,[2] Y. Amhis,[36] J. Anderson,[37] R. B. Appleby,[51] O. Aquines Gutierrez,[10] F. Archilli,[18,35] L. Arrabito,[55] A. Artamonov,[32] M. Artuso,[53,35] E. Aslanides,[6] G. Auriemma,[22,m] S. Bachmann,[11] J. J. Back,[45] D. S. Bailey,[51] V. Balagura,[28,35] W. Baldini,[16] R. J. Barlow,[51] C. Barschel,[35] S. Barsuk,[7] W. Barter,[44] A. Bates,[48] C. Bauer,[10] Th. Bauer,[38] A. Bay,[36] I. Bediaga,[1] S. Belogurov,[28] K. Belous,[32] I. Belyaev,[28] E. Ben-Haim,[8] M. Benayoun,[8] G. Bencivenni,[18] S. Benson,[47] J. Benton,[43] R. Bernet,[37] M.-O. Bettler,[17] M. van Beuzekom,[38] A. Bien,[11] S. Bifani,[12] T. Bird,[51] A. Bizzeti,[17,h] P. M. Bjørnstad,[51] T. Blake,[35] F. Blanc,[36] C. Blanks,[50] J. Blouw,[11] S. Blusk,[53] A. Bobrov,[31] V. Bocci,[22] A. Bondar,[31] N. Bondar,[27] W. Bonivento,[15] S. Borghi,[48,51] A. Borgia,[53] T. J. V. Bowcock,[49] C. Bozzi,[16] T. Brambach,[9] J. van den Brand,[39] J. Bressieux,[36] D. Brett,[51] M. Britsch,[10] T. Britton,[53] N. H. Brook,[43] H. Brown,[49] A. Büchler-Germann,[37] I. Burducea,[26] A. Bursche,[37] J. Buytaert,[35] S. Cadeddu,[15] O. Callot,[7] M. Calvi,[20,j] M. Calvo Gomez,[33,n] A. Camboni,[33] P. Campana,[18,35] A. Carbone,[14] G. Carboni,[21,k] R. Cardinale,[19,35,i] A. Cardini,[15] L. Carson,[50] K. Carvalho Akiba,[2] G. Casse,[49] M. Cattaneo,[35] Ch. Cauet,[9] M. Charles,[52] Ph. Charpentier,[35] N. Chiapolini,[37] K. Ciba,[35] X. Cid Vidal,[34] G. Ciezarek,[50] P. E. L. Clarke,[47,35] M. Clemencic,[35] H. V. Cliff,[44] J. Closier,[35] C. Coca,[26] V. Coco,[38] J. Cogan,[6] P. Collins,[35] A. Comerma-Montells,[33] F. Constantin,[26] A. Contu,[52] A. Cook,[43] M. Coombes,[43] G. Corti,[35] B. Couturier,[35] G. A. Cowan,[36] R. Currie,[47] C. D'Ambrosio,[35] P. David,[8] P. N. Y. David,[38] I. De Bonis,[4] S. De Capua,[21,k] M. De Cian,[37] F. De Lorenzi,[12] J. M. De Miranda,[1] L. De Paula,[2] P. De Simone,[18] D. Decamp,[4] M. Deckenhoff,[9] H. Degaudenzi,[36,35] L. Del Buono,[8] C. Deplano,[15] D. Derkach,[14,35] O. Deschamps,[5] F. Dettori,[39] J. Dickens,[44] H. Dijkstra,[35] P. Diniz Batista,[1] F. Domingo Bonal,[33,n] S. Donleavy,[49] F. Dordei,[11] A. Dosil Suárez,[34] D. Dossett,[45] A. Dovbnya,[40] F. Dupertuis,[36] R. Dzhelyadin,[32] A. Dziurda,[23] S. Easo,[46] U. Egede,[50] V. Egorychev,[28] S. Eidelman,[31] D. van Eijk,[38] F. Eisele,[11] S. Eisenhardt,[47] R. Ekelhof,[9] L. Eklund,[48] Ch. Elsasser,[37] D. Elsby,[42] D. Esperante Pereira,[34] L. Estève,[44] A. Falabella,[16,14,e] E. Fanchini,[20,j] C. Färber,[11] G. Fardell,[47] C. Farinelli,[38] S. Farry,[12] V. Fave,[36] V. Fernandez Albor,[34] M. Ferro-Luzzi,[35] S. Filippov,[30] C. Fitzpatrick,[47] M. Fontana,[10] F. Fontanelli,[19,i] R. Forty,[35] O. Francisco,[2] M. Frank,[35] C. Frei,[35] M. Frosini,[17,f] S. Furcas,[20] A. Gallas Torreira,[34] D. Galli,[14,c] M. Gandelman,[2] P. Gandini,[52] Y. Gao,[3] J-C. Garnier,[35] J. Garofoli,[53] J. Garra Tico,[44] L. Garrido,[33] D. Gascon,[33] C. Gaspar,[35] N. Gauvin,[36] M. Gersabeck,[35] T. Gershon,[45,35] Ph. Ghez,[4] V. Gibson,[44] V. V. Gligorov,[35] C. Göbel,[54] D. Golubkov,[28] A. Golutvin,[50,28,35] A. Gomes,[2] H. Gordon,[52] M. Grabalosa Gándara,[33] R. Graciani Diaz,[33] L. A. Granado Cardoso,[35] E. Graugés,[33] G. Graziani,[17] A. Grecu,[26] E. Greening,[52] S. Gregson,[44] B. Gui,[53] E. Gushchin,[30] Yu. Guz,[32] T. Gys,[35] G. Haefeli,[36] C. Haen,[35] S. C. Haines,[44] T. Hampson,[43] S. Hansmann-Menzemer,[11] R. Harji,[50] N. Harnew,[52] J. Harrison,[51] P. F. Harrison,[45] T. Hartmann,[56] J. He,[7] V. Heijne,[38] K. Hennessy,[49] P. Henrard,[5] J. A. Hernando Morata,[34] E. van Herwijnen,[35] E. Hicks,[49] K. Holubyev,[11] P. Hopchev,[4] W. Hulsbergen,[38] P. Hunt,[52] T. Huse,[49] R. S. Huston,[12] D. Hutchcroft,[49] D. Hynds,[48] V. Iakovenko,[41] P. Ilten,[12] J. Imong,[43] R. Jacobsson,[35] A. Jaeger,[11] M. Jahjah Hussein,[5] E. Jans,[38] F. Jansen,[38] P. Jaton,[36] B. Jean-Marie,[7] F. Jing,[3] M. John,[52] D. Johnson,[52] C. R. Jones,[44] B. Jost,[35] M. Kaballo,[9] S. Kandybei,[40] M. Karacson,[35] T. M. Karbach,[9] J. Keaveney,[12] I. R. Kenyon,[42] U. Kerzel,[35] T. Ketel,[39] A. Keune,[36] B. Khanji,[6] Y. M. Kim,[47] M. Knecht,[36] P. Koppenburg,[38] M. Korolev,[29] A. Kozlinskiy,[38] L. Kravchuk,[30] K. Kreplin,[11] M. Kreps,[45] G. Krocker,[11] P. Krokovny,[11] F. Kruse,[9] K. Kruzelecki,[35] M. Kucharczyk,[20,23,35,j] T. Kvaratskheliya,[28,35] V. N. La Thi,[36] D. Lacarrere,[35] G. Lafferty,[51] A. Lai,[15] D. Lambert,[47] R. W. Lambert,[39] E. Lanciotti,[35] G. Lanfranchi,[18] C. Langenbruch,[11] T. Latham,[45] C. Lazzeroni,[42] R. Le Gac,[6] J. van Leerdam,[38] J.-P. Lees,[4] R. Lefèvre,[5] A. Leflat,[29,35] J. Lefrançois,[7] O. Leroy,[6] T. Lesiak,[23] L. Li,[3] L. Li Gioi,[5] M. Lieng,[9] M. Liles,[49] R. Lindner,[35] C. Linn,[11] B. Liu,[3] G. Liu,[35] J. von Loeben,[20] J. H. Lopes,[2] E. Lopez Asamar,[33] N. Lopez-March,[36] H. Lu,[3] J. Luisier,[36] A. Mac Raighne,[48] F. Machefert,[7] I. V. Machikhiliyan,[4,28] F. Maciuc,[10] O. Maev,[27,35] J. Magnin,[1] S. Malde,[52] R. M. D. Mamunur,[35] G. Manca,[15,d] G. Mancinelli,[6] N. Mangiafave,[44] U. Marconi,[14] R. Märki,[36] J. Marks,[11] G. Martellotti,[22] A. Martens,[8] L. Martin,[52] A. Martín Sánchez,[7] D. Martinez Santos,[35] A. Massafferri,[1] Z. Mathe,[12] C. Matteuzzi,[20] M. Matveev,[27] E. Maurice,[6] B. Maynard,[53] A. Mazurov,[16,30,35] G. McGregor,[51] R. McNulty,[12] M. Meissner,[11] M. Merk,[38] J. Merkel,[9] R. Messi,[21,k] S. Miglioranzi,[35] D. A. Milanes,[13] M.-N. Minard,[4] J. Molina Rodriguez,[54] S. Monteil,[5] D. Moran,[12] P. Morawski,[23] R. Mountain,[53] I. Mous,[38] F. Muheim,[47] K. Müller,[37] R. Muresan,[26] B. Muryn,[24] B. Muster,[36] M. Musy,[33] J. Mylroie-Smith,[49] P. Naik,[43] T. Nakada,[36] R. Nandakumar,[46] I. Nasteva,[1] M. Nedos,[9] M. Needham,[47] N. Neufeld,[35] C. Nguyen-Mau,[36,o] M. Nicol,[7] V. Niess,[5] N. Nikitin,[29] A. Nomerotski,[52,35] A. Novoselov,[32] A. Oblakowska-Mucha,[24] V. Obraztsov,[32] S. Oggero,[38] S. Ogilvy,[48] O. Okhrimenko,[41] R. Oldeman,[15,35,d] M. Orlandea,[26] J. M. Otalora Goicochea,[2] P. Owen,[50] K. Pal,[53] J. Palacios,[37]

A. Palano,[13,b] M. Palutan,[18] J. Panman,[35] A. Papanestis,[46] M. Pappagallo,[48] C. Parkes,[51] C. J. Parkinson,[50] G. Passaleva,[17] G. D. Patel,[49] M. Patel,[50] S. K. Paterson,[50] G. N. Patrick,[46] C. Patrignani,[19,i] C. Pavel-Nicorescu,[26] A. Pazos Alvarez,[34] A. Pellegrino,[38] G. Penso,[22,l] M. Pepe Altarelli,[35] S. Perazzini,[14,c] D. L. Perego,[20,j] E. Perez Trigo,[34] A. Pérez-Calero Yzquierdo,[33] P. Perret,[5] M. Perrin-Terrin,[6] G. Pessina,[20] A. Petrella,[16,35] A. Petrolini,[19,i] A. Phan,[53] E. Picatoste Olloqui,[33] B. Pie Valls,[33] B. Pietrzyk,[4] T. Pilař,[45] D. Pinci,[22] R. Plackett,[48] S. Playfer,[47] M. Plo Casasus,[34] G. Polok,[23] A. Poluektov,[45,31] E. Polycarpo,[2] D. Popov,[10] B. Popovici,[26] C. Potterat,[33] A. Powell,[52] J. Prisciandaro,[36] V. Pugatch,[41] A. Puig Navarro,[33] W. Qian,[53] J. H. Rademacker,[43] B. Rakotomiaramanana,[36] M. S. Rangel,[2] I. Raniuk,[40] G. Raven,[39] S. Redford,[52] M. M. Reid,[45] A. C. dos Reis,[1] S. Ricciardi,[46] K. Rinnert,[49] D. A. Roa Romero,[5] P. Robbe,[7] E. Rodrigues,[48,51] F. Rodrigues,[2] P. Rodriguez Perez,[34] G. J. Rogers,[44] S. Roiser,[35] V. Romanovsky,[32] M. Rosello,[33,n] J. Rouvinet,[36] T. Ruf,[35] H. Ruiz,[33] G. Sabatino,[21,k] J. J. Saborido Silva,[34] N. Sagidova,[27] P. Sail,[48] B. Saitta,[15,d] C. Salzmann,[37] M. Sannino,[19,i] R. Santacesaria,[22] C. Santamarina Rios,[34] R. Santinelli,[35] E. Santovetti,[21,k] M. Sapunov,[6] A. Sarti,[18,l] C. Satriano,[22,m] A. Satta,[21] M. Savrie,[16,e] D. Savrina,[28] P. Schaack,[50] M. Schiller,[39] S. Schleich,[9] M. Schlupp,[9] M. Schmelling,[10] B. Schmidt,[35] O. Schneider,[36] A. Schopper,[35] M.-H. Schune,[7] R. Schwemmer,[35] B. Sciascia,[18] A. Sciubba,[18,l] M. Seco,[34] A. Semennikov,[28] K. Senderowska,[24] I. Sepp,[50] N. Serra,[37] J. Serrano,[6] P. Seyfert,[11] M. Shapkin,[32] I. Shapoval,[40,35] P. Shatalov,[28] Y. Shcheglov,[27] T. Shears,[49] L. Shekhtman,[31] O. Shevchenko,[40] V. Shevchenko,[28] A. Shires,[50] R. Silva Coutinho,[45] T. Skwarnicki,[53] A. C. Smith,[35] N. A. Smith,[49] E. Smith,[52,46] K. Sobczak,[5] F. J. P. Soler,[48] A. Solomin,[43] F. Soomro,[18,35] B. Souza De Paula,[2] B. Spaan,[9] A. Sparkes,[47] P. Spradlin,[48] F. Stagni,[35] S. Stahl,[11] O. Steinkamp,[37] S. Stoica,[26] S. Stone,[53,35] B. Storaci,[38] M. Straticiuc,[26] U. Straumann,[37] V. K. Subbiah,[35] S. Swientek,[9] M. Szczekowski,[25] P. Szczypka,[36] T. Szumlak,[24] S. T'Jampens,[4] E. Teodorescu,[26] F. Teubert,[35] C. Thomas,[52] E. Thomas,[35] J. van Tilburg,[11] V. Tisserand,[4] M. Tobin,[37] S. Topp-Joergensen,[52] N. Torr,[52] E. Tournefier,[4,50] M. T. Tran,[36] A. Tsaregorodtsev,[6] N. Tuning,[38] M. Ubeda Garcia,[35] A. Ukleja,[25] P. Urquijo,[53] U. Uwer,[11] V. Vagnoni,[14] G. Valenti,[14] R. Vazquez Gomez,[33] P. Vazquez Regueiro,[34] S. Vecchi,[16] J. J. Velthuis,[43] M. Veltri,[17,g] B. Viaud,[7] I. Videau,[7] D. Vieira,[2] X. Vilasis-Cardona,[33,n] J. Visniakov,[34] A. Vollhardt,[37] D. Volyanskyy,[10] D. Voong,[43] A. Vorobyev,[27] H. Voss,[10] S. Wandernoth,[11] J. Wang,[53] D. R. Ward,[44] N. K. Watson,[42] A. D. Webber,[51] D. Websdale,[50] M. Whitehead,[45] D. Wiedner,[11] L. Wiggers,[38] G. Wilkinson,[52] M. P. Williams,[45,46] M. Williams,[50] F. F. Wilson,[46] J. Wishahi,[9] M. Witek,[23] W. Witzeling,[35] S. A. Wotton,[44] K. Wyllie,[35] Y. Xie,[47] F. Xing,[52] Z. Xing,[53] Z. Yang,[3] R. Young,[47] O. Yushchenko,[32] M. Zangoli,[14] M. Zavertyaev,[10,a] F. Zhang,[3] L. Zhang,[53] W. C. Zhang,[12] Y. Zhang,[3] A. Zhelezov,[11] L. Zhong,[3] and A. Zvyagin[35]

(LHCb Collaboration)

[1]*Centro Brasileiro de Pesquisas Físicas (CBPF), Rio de Janeiro, Brazil*
[2]*Universidade Federal do Rio de Janeiro (UFRJ), Rio de Janeiro, Brazil*
[3]*Center for High Energy Physics, Tsinghua University, Beijing, China*
[4]*LAPP, Université de Savoie, CNRS/IN2P3, Annecy-Le-Vieux, France*
[5]*Clermont Université, Université Blaise Pascal, CNRS/IN2P3, LPC, Clermont-Ferrand, France*
[6]*CPPM, Aix-Marseille Université, CNRS/IN2P3, Marseille, France*
[7]*LAL, Université Paris-Sud, CNRS/IN2P3, Orsay, France*
[8]*LPNHE, Université Pierre et Marie Curie, Université Paris Diderot, CNRS/IN2P3, Paris, France*
[9]*Fakultät Physik, Technische Universität Dortmund, Dortmund, Germany*

[a]P.N. Lebedev Physical Institute, Russian Academy of Science (LPI RAS), Moscow, Russia
[b]Università di Bari, Bari, Italy
[c]Università di Bologna, Bologna, Italy
[d]Università di Cagliari, Cagliari, Italy
[e]Università di Ferrara, Ferrara, Italy
[f]Università di Firenze, Firenze, Italy
[g]Università di Urbino, Urbino, Italy
[h]Università di Modena e Reggio Emilia, Modena, Italy
[i]Università di Genova, Genova, Italy
[j]Università di Milano Bicocca, Milano, Italy
[k]Università di Roma Tor Vergata, Roma, Italy
[l]Università di Roma La Sapienza, Roma, Italy
[m]Università della Basilicata, Potenza, Italy
[n]LIFAELS, La Salle, Universitat Ramon Llull, Barcelona, Spain
[o]Hanoi University of Science, Hanoi, Viet Nam

[10]Max-Planck-Institut für Kernphysik (MPIK), Heidelberg, Germany

[11]Physikalisches Institut, Ruprecht-Karls-Universität Heidelberg, Heidelberg, Germany

[12]School of Physics, University College Dublin, Dublin, Ireland

[13]Sezione INFN di Bari, Bari, Italy

[14]Sezione INFN di Bologna, Bologna, Italy

[15]Sezione INFN di Cagliari, Cagliari, Italy

[16]Sezione INFN di Ferrara, Ferrara, Italy

[17]Sezione INFN di Firenze, Firenze, Italy

[18]Laboratori Nazionali dell'INFN di Frascati, Frascati, Italy

[19]Sezione INFN di Genova, Genova, Italy

[20]Sezione INFN di Milano Bicocca, Milano, Italy

[21]Sezione INFN di Roma Tor Vergata, Roma, Italy

[22]Sezione INFN di Roma La Sapienza, Roma, Italy

[23]Henryk Niewodniczanski Institute of Nuclear Physics Polish Academy of Sciences, Kraków, Poland

[24]AGH University of Science and Technology, Kraków, Poland

[25]Soltan Institute for Nuclear Studies, Warsaw, Poland

[26]Horia Hulubei National Institute of Physics and Nuclear Engineering, Bucharest-Magurele, Romania

[27]Petersburg Nuclear Physics Institute (PNPI), Gatchina, Russia

[28]Institute of Theoretical and Experimental Physics (ITEP), Moscow, Russia

[29]Institute of Nuclear Physics, Moscow State University (SINP MSU), Moscow, Russia

[30]Institute for Nuclear Research of the Russian Academy of Sciences (INR RAN), Moscow, Russia

[31]Budker Institute of Nuclear Physics (SB RAS) and Novosibirsk State University, Novosibirsk, Russia

[32]Institute for High Energy Physics (IHEP), Protvino, Russia

[33]Universitat de Barcelona, Barcelona, Spain

[34]Universidad de Santiago de Compostela, Santiago de Compostela, Spain

[35]European Organization for Nuclear Research (CERN), Geneva, Switzerland

[36]Ecole Polytechnique Fédérale de Lausanne (EPFL), Lausanne, Switzerland

[37]Physik-Institut, Universität Zürich, Zürich, Switzerland

[38]Nikhef National Institute for Subatomic Physics, Amsterdam, The Netherlands

[39]Nikhef National Institute for Subatomic Physics and Vrije Universiteit, Amsterdam, The Netherlands

[40]NSC Kharkiv Institute of Physics and Technology (NSC KIPT), Kharkiv, Ukraine

[41]Institute for Nuclear Research of the National Academy of Sciences (KINR), Kyiv, Ukraine

[42]University of Birmingham, Birmingham, United Kingdom

[43]H. H. Wills Physics Laboratory, University of Bristol, Bristol, United Kingdom

[44]Cavendish Laboratory, University of Cambridge, Cambridge, United Kingdom

[45]Department of Physics, University of Warwick, Coventry, United Kingdom

[46]STFC Rutherford Appleton Laboratory, Didcot, United Kingdom

[47]School of Physics and Astronomy, University of Edinburgh, Edinburgh, United Kingdom

[48]School of Physics and Astronomy, University of Glasgow, Glasgow, United Kingdom

[49]Oliver Lodge Laboratory, University of Liverpool, Liverpool, United Kingdom

[50]Imperial College London, London, United Kingdom

[51]School of Physics and Astronomy, University of Manchester, Manchester, United Kingdom

[52]Department of Physics, University of Oxford, Oxford, United Kingdom

[53]Syracuse University, Syracuse, New York, USA

[54]Pontifícia Universidade Católica do Rio de Janeiro (PUC-Rio), Rio de Janeiro, Brazil,
associated to Universidade Federal do Rio de Janeiro (UFRJ), Rio de Janeiro, Brazil

[55]CC-IN2P3, CNRS/IN2P3, Lyon-Villeurbanne, France, associated member

[56]Physikalisches Institut, Universität Rostock, Rostock, Germany,
associated to Physikalisches Institut, Ruprecht-Karls-Universität Heidelberg, Heidelberg, Germany

A search for the $X(4140)$ state in $B^+ \rightarrow J/\psi \phi K^+$ decays is performed with 0.37 fb^{-1} of pp collisions at $\sqrt{s} = 7$ TeV collected by the LHCb experiment. No evidence for this state is found, in 2.4σ disagreement with a measurement by CDF. An upper limit on its production rate is set, $\mathcal{B}(B^+ \rightarrow X(4140)K^+) \times \mathcal{B}(X(4140) \rightarrow J/\psi \phi)/\mathcal{B}(B^+ \rightarrow J/\psi \phi K^+) < 0.07$ at 90% confidence level.

In this article, results are presented from the search for the narrow $X(4140)$ resonance decaying to $J/\psi\phi$ using $B^+ \rightarrow J/\psi\phi K^+$ events [1] ($J/\psi \rightarrow \mu^+\mu^-$, $\phi \rightarrow K^+K^-$), in a data sample corresponding to an integrated luminosity of 0.37 fb^{-1} collected in pp collisions at the LHC at $\sqrt{s} = 7$ TeV using the LHCb detector. The CDF collaboration reported a 3.8σ evidence for the $X(4140)$ state (also referred to as $Y(4140)$ in the literature) in these decays using $p\bar{p}$ data collected at the Tevatron ($\sqrt{s} = 1.96$ TeV) [2]. A preliminary update of the CDF analysis with 6.0 fb^{-1} reported 115 ± 12 $B^+ \rightarrow J/\psi\phi K^+$ events and 19 ± 6 $X(4140)$ candidates leading to a statistical significance of more than 5σ [3]. The mass and width were determined to be $4143.4^{+2.9}_{-3.0} \pm 0.6$ MeV and $15.3^{+10.4}_{-6.1} \pm 2.5$ MeV, respectively[4]. The relative branching ratio was measured to be $\mathcal{B}(B^+ \rightarrow X(4140)K^+) \times \mathcal{B}(X(4140) \rightarrow J/\psi\phi)/\mathcal{B}(B^+ \rightarrow J/\psi\phi K^+) = 0.149 \pm 0.039 \pm 0.024$.

Charmonium states at this mass are expected to have much larger widths because of open flavour decay channels [5]. Thus, their decay rate into the $J/\psi\phi$ mode, which is near the kinematic threshold, should be small and unobservable. Therefore, the observation by CDF has triggered wide interest among model builders of exotic hadronic states. It has been suggested that the $X(4140)$ resonance could be a molecular state [6–12], a tetraquark state [13,14], a hybrid state [15,16] or a rescattering effect [17,18]. The Belle experiment found no evidence for the $X(4140)$ state in the $\gamma\gamma \rightarrow J/\psi\phi$ process, which disfavored the molecular interpretation [19]. The CDF data also suggested that there could be a second state at a mass of $4274.4^{+8.4}_{-6.4} \pm 1.9$ MeV with a width of $32.3^{+21.9}_{-15.3} \pm 7.6$ MeV [3]. In this case, the event yield was 22 ± 8 with 3.1σ significance. This observation has also received attention in the literature [20,21].

The LHCb detector [22] is a single-arm forward spectrometer covering the pseudorapidity range $2 < \eta < 5$, designed for the study of particles containing b or c quarks. The detector includes a high precision tracking system consisting of a silicon-strip vertex detector surrounding the pp interaction region, a large-area silicon-strip detector located upstream of a dipole magnet with a bending power of about 4 Tm, and three stations of silicon-strip detectors and straw drift-tubes placed downstream. The combined tracking system has a momentum resolution $\Delta p/p$ that varies from 0.4% at 5 GeV/c to 0.6% at 100 GeV/c, and an impact parameter (IP) resolution of 20 μm for tracks with high transverse momentum. Charged hadrons are identified using two ring-imaging Cherenkov detectors. Photon, electron and hadron candidates are identified by a calorimeter system consisting of scintillating-pad and preshower detectors, an electromagnetic calorimeter (ECAL) and a hadronic calorimeter (HCAL). Muons are identified by a muon system (MUON) composed of alternating layers of iron and multiwire proportional chambers. The MUON, ECAL and HCAL provide the capability of first-level hardware triggering. The single and dimuon hardware triggers provide good efficiency for $B^+ \rightarrow J/\psi\phi K^+$, $J/\psi \rightarrow \mu^+\mu^-$ events. Events passing the hardware trigger are read out and sent to an event filter farm for further processing. Here, a software based two-stage trigger reduces the rate from 1 MHz to about 3 kHz. The most efficient software triggers [23] for this analysis require a charged track with transverse momentum (p_T) of more than 1.7 GeV ($p_T > 1.0$ GeV if identified as muon) and with an IP to any primary pp-interaction vertex (PV) larger than 100 μm. A dimuon trigger requiring $p_T(\mu) > 0.5$ GeV, large dimuon mass, $M(\mu^+\mu^-) > 2.7$ GeV, and with no IP requirement complements the single track triggers. At final stage, we either require a $J/\psi \rightarrow \mu^+\mu^-$ candidate with $p_T > 1.5$ GeV or a muon-track pair with significant IP.

In the subsequent offline analysis, $J/\psi \rightarrow \mu^+\mu^-$ candidates are selected with the following criteria: $p_T(\mu) > 0.9$ GeV, χ^2 per degree of freedom of the two muons forming a common vertex, $\chi^2_{vtx}(\mu^+\mu^-)/$ndf < 9, and a mass window $3.04 < M(\mu^+\mu^-) < 3.14$ GeV. We then find $K^+K^-K^+$ combinations consistent with originating from a common vertex with $\chi^2_{vtx}(K^+K^-K^+)/$ndf < 9. Every charged track with $p_T > 0.25$ GeV, missing all PVs by at least 3 standard deviations ($\chi^2_{IP}(K) > 9$) and classified more likely to be a kaon than a pion according to the particle identification system, is considered a kaon candidate [24]. A five-track $J/\psi K^+K^-K^+$ vertex is formed ($\chi^2_{vtx}(J/\psi K^+K^-K^+)/$ndf < 9). This B^+ candidate is required to have $p_T > 4.0$ GeV and a decay time as measured with respect to the PV of at least 0.25 ps. When more than one PV is reconstructed, the one that gives the smallest IP significance for the B^+ candidate is chosen. The invariant mass of a $\mu^+\mu^-K^+K^-K^+$ combination is evaluated after the muon pair is constrained to the J/ψ mass, and all final state particles are constrained to a common vertex.

Further background suppression is provided by a likelihood ratio. In the case of uncorrelated input variables this provides the most efficient discrimination between signal and background. The overall likelihood is a product of probability density functions, $\mathcal{P}(x_i)$ (PDFs), for the four sensitive variables (x_i): smallest $\chi^2_{IP}(K)$ among the kaon candidates, $\chi^2_{vtx}(J/\psi K^+K^-K^+)/$ndf, B candidate IP significance, $\chi^2_{IP}(B)$, and cosine of the largest opening angle between the J/ψ and kaon candidates in the plane transverse to the beam. The latter peaks towards $+1$ for the signal as the B^+ meson has a high transverse momentum. Backgrounds combining particles from two different B mesons peak at -1. Backgrounds including other random combinations are uniformly distributed. The signal PDFs, $\mathcal{P}_{sig}(x_i)$, are obtained from the phase-space simulation of $B^+ \rightarrow J/\psi\phi K^+$ decays. The background PDFs, $\mathcal{P}_{bkg}(x_i)$, are obtained from the data candidates with $J/\psi K^+K^-K^+$ invariant mass between 5.6 and 6.4 GeV (far-sideband).

A logarithm of the ratio of the signal and background PDFs is formed: $\mathrm{DLL}_{\mathrm{sig/bkg}} = -2\sum_i^4 \ln(\mathcal{P}_{\mathrm{sig}}(x_i)/\mathcal{P}_{\mathrm{bkg}}(x_i))$. A requirement on the log-likelihood ratio, $\mathrm{DLL}_{\mathrm{sig/bkg}} < -1$, has been chosen by maximizing $N_{\mathrm{sig}}/\sqrt{N_{\mathrm{sig}} + N_{\mathrm{bkg}}}$, where N_{sig} is the expected $B^+ \to J/\psi K^+ K^- K^+$ signal yield and the N_{bkg} is the background yield in the B^+ peak region ($\pm 2.5\sigma$). The absolute normalization of N_{sig} and N_{bkg} comes from a fit to the $J/\psi \phi K$ invariant mass distribution with $\mathrm{DLL}_{\mathrm{sig/bkg}} < 0$, while their dependence on the $\mathrm{DLL}_{\mathrm{sig/bkg}}$ requirement comes from the signal simulation and the far-sideband, respectively.

The $J/\psi \phi K$ invariant mass distribution, with a requirement that at least one $K^+ K^-$ combination has an invariant mass within ± 15 MeV of the ϕ mass, is shown in Fig. 1. A fit to a Gaussian and a quadratic function in the range 5.1–5.5 GeV results in 346 ± 20 B^+ events with a mass resolution of 5.2 ± 0.3 MeV. Alternatively requiring the invariant mass $M(J/\psi K^+ K^- K^+)$ to be within ± 2.5 standard deviations of the observed B^+ peak position, we fit the $M(K^+ K^-)$ mass distribution (two combinations per event) using a binned maximum likelihood fit with a P-wave relativistic Breit-Wigner representing the $\phi(1020)$ and a two-body phase-space distribution to represent combinatorial background, both convolved with a Gaussian mass resolution. The ϕ resonance width is fixed to the PDG value (4.26 MeV) [25]. The $M(K^+ K^-)$ mass distribution is displayed in Fig. 2 with the fit results overlaid. The fitted parameters are the ϕ yield, the ϕ mass (1019.3 ± 0.2 MeV), the background yield and the mass resolution (1.4 ± 0.3 MeV). The fit neglects a possible interference of the ϕ resonance with nonresonant $K^+ K^-$ background. Replacing the two-body phase-space function by a third-order polynomial does not change the results. In order to subtract a non-B contribution, we fit the $M(K^+ K^-)$
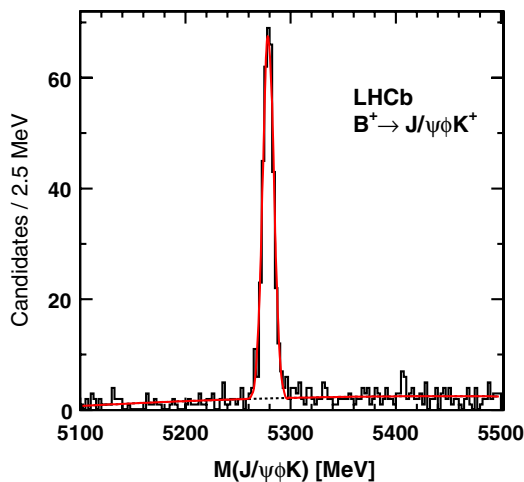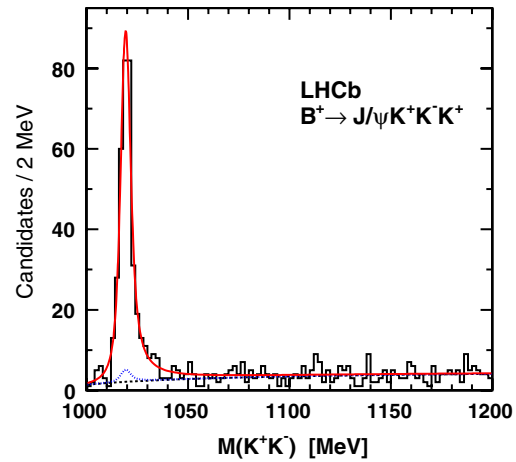

FIG. 2 (color online). Invariant $M(K^+ K^-)$ mass distribution selecting $B^+ \to J/\psi K^+ K^- K^+$ events in the $\pm 2.5\sigma$ region around the B^+ mass peak. The dashed line shows the two-body phase-space contribution. The small blue dotted ϕ peak on top of it illustrates the amount of the background ϕ mesons estimated from the fit to the B^+ mass near-sidebands.

distribution from the B mass near-sidebands (from 4 to 14 standard deviations on either side) leaving only the ϕ yield and the two-body phase-space background yield as free parameters. After scaling to the signal region, this leads to 14 ± 3 background events. The background subtracted $B^+ \to J/\psi \phi K^+$ yield ($N_{B^+ \to J/\psi \phi K^+}$) is 382 ± 22 events.

To search for the $X(4140)$ state, we select events within ± 15 MeV of the ϕ mass. According to the fit to the $M(K^+ K^-)$ distribution this requirement is 85% efficient. Figure 3 shows the mass difference $M(J/\psi \phi) - M(J/\psi)$ distribution (no J/ψ or ϕ mass constraints have been used). No narrow structure is observed near the threshold. We employ the fit model used by CDF [3] to quantify the compatibility of the two measurements. The data are fitted with a spin-zero relativistic Breit-Wigner shape together with a three-body phase-space function ($\mathcal{F}_1^{\mathrm{bkg}}$), both convolved with the detector resolution. The efficiency dependence is extracted from simulation (Fig. 4) and applied as a shape correction to the three-body phase-space and the Breit-Wigner function. The mass and width of the $X(4140)$ peak are fixed to the central values obtained by the CDF collaboration. The mass-difference resolution was determined from the $B^+ \to X(4140)K^+$ simulation to be 1.5 ± 0.1 MeV. A binned maximum likelihood fit of the signal and background yields is shown in Fig. 3(a). The region above 1400 MeV is excluded since it is more likely to contain non $B^+ \to J/\psi \phi K^+$ backgrounds. By excluding also the region below 1030 MeV, where the three-body phase-space and signal yields are very small (0.5% and 3.5% of the yields included in the fit, respectively), we make our results less vulnerable to possible small contributions from the other sources. The fit shown in Fig. 3(a) gives a $X(4140)$ yield of 6.9 ± 4.9 events. Fitting the

FIG. 1 (color online). Mass distribution for $B^+ \to J/\psi \phi K^+$ candidates in the data after the ± 15 MeV ϕ mass requirement. The fit of a Gaussian signal with a quadratic background (dashed line) is superimposed (solid red line).
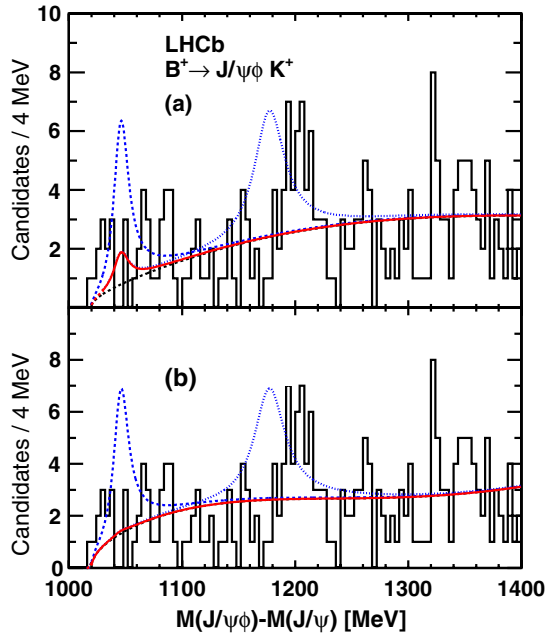
FIG. 3 (color online). Distribution of the mass difference $M(J/\psi\phi) - M(J/\psi)$ for the $B^+ \rightarrow J/\psi\phi K^+$ in the B^+ ($\pm$ 2.5σ) and ϕ ($\pm$ 15 MeV) mass windows. Fit of $X(4140)$ signal on top of a smooth background is superimposed (solid red line). The dashed blue (dotted blue) line on top illustrates the expected $X(4140)$ ($X(4274)$) signal yield from the CDF measurement [3]. The top and bottom plots differ by the background function (dashed black line) used in the fit: (a) an efficiency-corrected three-body phase-space ($\mathcal{F}_1^{\text{bkg}}$); (b) a quadratic function multiplied by the efficiency-corrected three-body phase-space factor ($\mathcal{F}_2^{\text{bkg}}$). The fit ranges are 1030–1400 and 1020–1400 MeV, respectively.

second state at a mass of 4274.44 MeV and with a width of 32.3 MeV [3] does not affect the $X(4140)$ yield. Reflections of $K\phi$ resonances [26,27] and possible broad $J/\psi\phi$ resonances can also contribute near and under the narrow $X(4140)$ resonance. To explore the sensitivity of our results to the assumed background shape, we also fit the data in the 1020–1400 MeV range with a quadratic function multiplied by the efficiency-corrected three-body phase-space factor ($\mathcal{F}_2^{\text{bkg}}$) to impose the kinematic threshold. The preferred value of the $X(4140)$ yield is 0.6 events with a positive error of 7.1 events. This fit is shown in Fig. 3(b).

A similar fit was performed to simulated $B^+ \rightarrow X(4140)K^+$ data to estimate the efficiency for this channel. The efficiency ratio between this fit and the ϕ signal fit to the $B^+ \rightarrow J/\psi\phi K^+$ events distributed according to the phase-space model, $\epsilon(B^+ \rightarrow X(4140)K^+, X(4140) \rightarrow J/\psi\phi)/\epsilon(B^+ \rightarrow J/\psi\phi K^+)$, was determined to be 0.62 ± 0.04 and includes the efficiency of the ϕ mass window requirement. Using our $B^+ \rightarrow J/\psi\phi K^+$ yield multiplied by this efficiency ratio and by the CDF value for $\mathcal{B}(B^+ \rightarrow X(4140)K^+)/\mathcal{B}(B^+ \rightarrow J/\psi\phi K^+)$ [3], leads to a prediction that we should have observed $35 \pm 9 \pm 6$ events, where the first uncertainty is statistical from the CDF
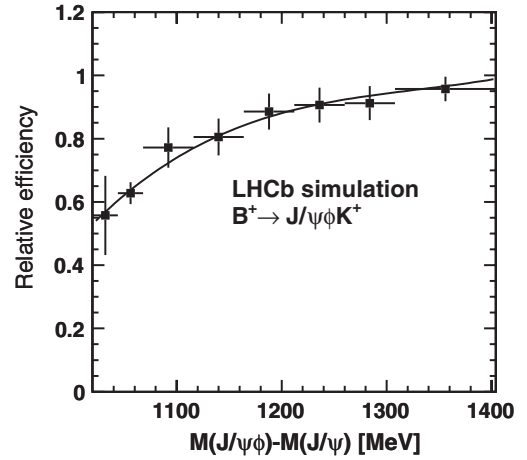

FIG. 4. Efficiency dependence on $M(J/\psi\phi) - M(J/\psi)$ as determined from the simulation (points with error bars). The efficiency is normalized with respect to the efficiency of the ϕ signal fit to the $B^+ \rightarrow J/\psi\phi K^+$ events distributed according to the phase-space model. A cubic polynomial was fitted to the simulated data (superimposed).

data and the second includes both the CDF and LHCb systematic uncertainties. Given the B^+ yield and relative efficiency, our sensitivity to the $X(4140)$ signal is a factor of 2 better than that of the CDF. The central value of this estimate is shown as a dashed line in Fig. 3. Taking the statistical and systematic errors from both experiments into account, our results disagree with the CDF observation by 2.4σ (2.7σ) when using $\mathcal{F}_1^{\text{bkg}}$ ($\mathcal{F}_2^{\text{bkg}}$) background shapes.

Since no evidence for the $X(4140)$ state is found, we set an upper limit on its production. Using a Bayesian approach, we integrate the fit likelihood determined as a function of the $X(4140)$ yield and find an upper limit on the number of signal events of 16 (13) at 90% confidence level (CL) for the two background shapes. Dividing the least stringent limit on the signal yield by the $B^+ \rightarrow J/\psi\phi K^+$ yield and $\epsilon(B^+ \rightarrow X(4140)K^+)/\epsilon(B^+ \rightarrow J/\psi\phi K^+)$ gives a limit on $\mathcal{B}(B^+ \rightarrow X(4140)K^+) \times \mathcal{B}(X(4140) \rightarrow J/\psi\phi)/\mathcal{B}(B^+ \rightarrow J/\psi\phi K^+)$. The systematic uncertainty on $\epsilon(B^+ \rightarrow X(4140)K^+)/\epsilon(B^+ \rightarrow J/\psi\phi K^+)$ is 6%. This uncertainty includes the statistical error from the simulation as well as the observed differences in track reconstruction efficiency between the simulation and data measured with the inclusive $J/\psi \rightarrow \mu^+\mu^-$ signal. Fit systematics related to the detector resolution and the uncertainty in the shape of the efficiency dependence on the $J/\psi\phi$ mass were also studied and found to be small. We multiply our limit by 1.06 and obtain at 90% CL

$$\frac{\mathcal{B}(B^+ \rightarrow X(4140)K^+) \times \mathcal{B}(X(4140) \rightarrow J/\psi\phi)}{\mathcal{B}(B^+ \rightarrow J/\psi\phi K^+)} < 0.07.$$

We also set an upper limit on the $X(4274)$ state suggested by the CDF collaboration [3]. The fit with $\mathcal{F}_1^{\text{bkg}}$ background shape gives $3.4^{+6.5}_{-3.4}$ events at this mass. The fit

with the $\mathcal{F}_2^{\mathrm{bkg}}$ background shape gives zero signal events with a positive error of 10. Integration of the fit likelihoods gives <24 and <20 events at 90% CL, respectively. The relative efficiency at this mass is $\epsilon(B^+ \to X(4274)K^+$, $X(4274) \to J/\psi\phi)/\epsilon(B^+ \to J/\psi\phi K^+) = 0.86 \pm 0.10$. The least stringent limit on the signal events yields an upper limit of

$$\frac{\mathcal{B}(B^+ \to X(4274)K^+) \times \mathcal{B}(X(4274) \to J/\psi\phi)}{\mathcal{B}(B^+ \to J/\psi\phi K^+)} < 0.08$$

at 90% CL, which includes the systematic uncertainty. CDF did not provide a measurement of this ratio of branching fractions. Assuming the efficiency is similar for the $X(4274)$ and $X(4140)$ resonances, their $X(4274)$ event yield corresponds to $\mathcal{B}(B^+ \to X(4274)K^+) \times \mathcal{B}(X(4274) \to J/\psi\phi)/\mathcal{B}(B^+ \to J/\psi\phi K^+) = 0.17 \pm 0.06$ (statistical uncertainty only). Scaling to our data, we should have observed 53 ± 19 $X(4274)$ events, which is illustrated in Fig. 3.

In summary, the most sensitive search for the narrow $X(4140) \to J/\psi\phi$ state just above the kinematic threshold

in $B^+ \to J/\psi\phi K^+$ decays has been performed using 0.37 fb^{-1} of data collected with the LHCb detector. We do not confirm the existence of such a state. Our results disagree at the 2.4σ level with the CDF measurement. An upper limit on $\mathcal{B}(B^+ \to X(4140)K^+) \times \mathcal{B}(X(4140) \to J/\psi\phi))/\mathcal{B}(B^+ \to J/\psi\phi K^+)$ of <0.07 at 90% CL is set.

[1] Charge-conjugate states are implied in this paper.
[2] T. Aaltonen *et al.* (CDF Collaboration), Phys. Rev. Lett. **102**, 242002 (2009).
[3] T. Aaltonen *et al.* (CDF Collaboration), arXiv:1101.6058.
[4] Units in which $c = 1$ are used.
[5] N. Brambilla *et al.*, Eur. Phys. J. C **71**, 1534 (2011).
[6] X. Liu and S.-L. Zhu, Phys. Rev. D **80**, 017502 (2009).
[7] T. Branz, T. Gutsche, and V. E. Lyubovitskij, Phys. Rev. D **80**, 054019 (2009).
[8] R. M. Albuquerque, M. E. Bracco, and M. Nielsen, Phys. Lett. B **678**, 186 (2009).
[9] G.-J. Ding, Eur. Phys. J. C **64**, 297 (2009).
[10] J.-R. Zhang and M.-Q. Huang, J. Phys. G **37**, 025005 (2010).
[11] X. Liu and H.-W. Ke, Phys. Rev. D **80**, 034009 (2009).
[12] Z.-G. Wang, Z.-C. Liu, and X.-H. Zhang, Eur. Phys. J. C **64**, 373 (2009).
[13] F. Stancu, J. Phys. G **37**, 075017 (2010).
[14] N. V. Drenska, R. Faccini, and A. D. Polosa, Phys. Rev. D **79**, 077502 (2009).
[15] N. Mahajan, Phys. Lett. B **679**, 228 (2009).

[16] Z.-G. Wang, Eur. Phys. J. C **63**, 115 (2009).
[17] X. Liu, Phys. Lett. B **680**, 137 (2009).
[18] D. V. Bugg, arXiv:1103.5363.
[19] C. Shen *et al.* (Belle Collaboration), Phys. Rev. Lett. **104**, 112004 (2010).
[20] J. He and X. Liu, arXiv:1102.1127.
[21] S. I. Finazzo, M. Nielsen, and X. Liu, Phys. Lett. B **701**, 101 (2011).
[22] A. A. Alves Jr *et al.* (LHCb Collaboration), JINST **3**, S08005 (2008).
[23] V. Gligorov, C. Thomas, and M. Williams, Report No. LHCb-PUB-2011-016.
[24] After all other selection criteria, the kaon identification cut is 94% efficient for the simulated $B^+ \to J/\psi K^+ K^- K^+$ events, and reduces the background under the B mass peak by a factor of 19.
[25] K. Nakamura *et al.* (Particle Data Group), J. Phys. G **37**, 075021 (2010).
[26] D. Frame *et al.*, Nucl. Phys. **B276**, 667 (1986).
[27] T. Armstrong *et al.* (Bari-Birmingham-CERN-Milan-Paris-Pavia Collaboration), Nucl. Phys. **B221**, 1 (1983).